Adaptive Image Deringing

Andrey V. Nasonov, Andrey S. Krylov
Laboratory of Mathematical Methods of Image Processing,
Faculty of Computational Mathematics and Cybernetics, Lomonosov Moscow State University,
{nasonov, kryl}@cs.msu.ru

Abstract

This paper proposes new and original adaptive image ringing detection and ringing suppression methods. Ringing detection is performed using a scale-space based computational analysis of ideal low-pass filtering of step edges. Edge width conception is introduced and is used to approximate ringing parameter. Method to choose strong isolated edges which are the best suitable edges for ringing analysis is proposed. A method of ringing level estimation for 2D images with unknown ringing parameters is introduced and used to perform real image deringing. New image quality metrics sensible to ringing artifact are introduced and used to analyze image resampling methods.

Keywords: *Ringing estimation, total variation, scale space, adaptive deringing.*

1. INTRODUCTION

Development of image enhancement methods is one of the most important image processing tasks. Ringing effect (Gibbs phenomenon) appears in images as oscillations near sharp edges. It is a result of a cut-off of high-frequency information. Ringing can appear as a result of image compression, image upsampling and other applications. An example of this effect can be seen in old video stored in analog format (Fig.1).

One of the main problems of image deringing is to detect the presence of ringing effect and to estimate the necessary ringing suppression level. But there is no algorithm which estimates ringing level in the general case.

There are image ringing estimation algorithms to measure ringing effect for a specific problem. In [1] wavelet decomposition is used and ringing effect is measured for JPEG-2000 compression as a difference between correlations of neighbor coefficients of different wavelet subbands. The problem of image deringing after JPEG-2000 compression is also considered in [2], [3].

Some metrics were developed to control image deringing as a post-processing. Regularization parameter estimation for image deringing using MAP approach is proposed in [4]. For the problem of image deringing after resampling, regularization parameter is estimated using information on the initial low resolution image [5]. In [6], the ringing metrics is defined as maximum of the differences between pixel values of the reference image and the processed image in the edge neighborhood. The size of this neighborhood is fixed a priori. In [7], the presence of ringing effect is detected by comparing the directions of image gradients at different scales.

The work [8] does not introduce a ringing estimation method, but it presents an algorithm to find regions where the ringing effect is the most visible. It is based on luminance masking and texture masking as typical for the human visual system.

In [9], a no-reference ringing detection method using Gabor filtering was suggested. It shows good results but it fails if image contains periodic structures like fence, geometrical textures, etc.

Figure 1: A video frame with a strong ringing effect.

In this article, we suggest new general ringing estimation algorithm based on total variation (TV) control. The TV was first used in image enhancement by Rudin, Osher and Fatemi [10] for image denoising. General relations between TV and ringing effect can be found in [11].

The rest of the paper is organized as follows. In section 2, we perform scale-space analysis of ringing effect and present a method of ringing level estimation for 1D edges with known ringing parameters. In section 3, we introduce a method of ringing level estimation for 2D images with unknown ringing parameters and an algorithm of strong isolated edges selection to choose the best suitable edges for ringing analysis. In section 4, we propose image quality metrics to compare different image restoration methods. In section 5, we suggest methods of ringing suppression for the problem of ringing reduction after interpolation and for the problem of blind image deringing. Section 6 concludes the paper.

2. 1D EDGE RINGING EFFECT ANALYSIS

We start from experimental analysis of one-dimensional edges with manually generated ringing artifact with known ringing parameters. The analysis consists of Total Variation (TV) calculation of edges convolved with Gauss filter with different radiuses.

2.1 Total Variation

In one-dimensional case, Total Variation functional is defined as

$$TV(f) = \int_{-\infty}^{\infty} |f'(x)|dx.$$

In a discrete case $-\infty < \ldots < x_{k-1} < x_k < \ldots < \infty$, it looks as:

$$TV(f) = \sum_{k=-\infty}^{\infty} |f(x_k) - f(x_{k-1})|.$$

We also consider weighted TV (WTV) with weight function $w(x)$:

$$TV(f, w) = \int_{-\infty}^{\infty} |f'(x)|w(x)dx.$$

In the discrete case it looks as

$$TV(f,w) = \sum_{k=-\infty}^{\infty} |f(x_k) - f(x_{k-1})| w\left(\frac{x_{k-1}+x_k}{2}\right).$$

2.2 Ringing Model

We consider the problem of ringing level estimation for ideal step edge (ISE)

$$\overline{f}(x) = \begin{cases} 1, & x \geq 0, \\ 0, & x < 0. \end{cases}$$

In the discrete case, $TV(\overline{f}) = 1$ for any grid.

Ringing effect can be generated by ideal low-pass filter which truncates high frequency data. We implement it using sinc interpolation of ideal step edge function $\overline{f}(x)$ given at the discrete set $\{x_k\}, x_k = dk + \frac{d}{2}$:

$$f_d(x) = \sum_k \overline{f}(x_k) \mathrm{sinc} \frac{x - x_k}{d}, \tag{1}$$

where $\mathrm{sinc}(x) = \frac{\sin \pi x}{\pi x}$. We call here the value d as ringing half-period. We call here the value d as quasiperiod of ringing oscillations. This value is in inverse proportion to the signal bandwidth.

Real edges are corrupted by noise, so this fact is to be considered too. In this work, we analyze the case of additive uniform noise $f_{d,n}(x) = f_d(x) + \xi_n(x)$, $f_n(x) = \overline{f}(x) + \xi_n(x)$, where $\xi_n(x)$ is uniformly distributed random function which values are in $(-n/2, n/2)$ range. We consider $n \leq n_0$, where n_0 is the maximum noise value.

2.3 Scale-space TV Analysis

We performed an experimental analysis of TV of edges with different quasiperiods d at different scales σ. Real edges are not infinite. To take into account only several first ringing oscillations, we use weighted TV with Gaussian weight $w_{\alpha d}(x) = e^{-\frac{x^2}{2(\alpha d)^2}}$, where α controls the number of considered ringing oscillations. To find the differences between edges with ringing effect and edges without it, we analyze the functional

$$TV(f, \sigma, w_{\alpha d}) = TV(f * G_\sigma, w_{\alpha d}),$$

where $f * G_\sigma$ is a convolution of f with Gauss filter with radius σ.

To design an algorithm to find the value σ_0 that best discriminates between edges with ringing artifact and edges without ringing artifact for fixed d, fixed maximum noise level n_0 and given parameter α, the following analysis has been performed:

We generated a large number (about 1000) of edges with and without ringing effect and with random noise levels $0 \leq n \leq n_0$ for the analysis. For every σ, we found the maximal value of TV functional for step edges without ringing effect

$$g_*(\sigma, d) = \max_{f_n} TV(f_n, \sigma, w_{\alpha d})$$

and the minimal value of TV functional for step edges with ringing effect

$$g^*(\sigma, d) = \min_{f_{d,n}} TV(f_{d,n}, \sigma, w_{\alpha d}).$$

The higher noise level is, the higher is the value of edge TV. Thus, to calculate $g_*(\sigma, d)$, we used only step edges f_n with the maximum noise level $n = n_0$

$$g_*(\sigma, d) = \max_{f_{n_0}} TV(f_{n_0}, \sigma, w_{\alpha d})$$

and for $g^*(\sigma, d)$ calculation, we uses only step edge f_d without noise

$$g^*(\sigma, d) = TV(f_d, \sigma, w_{\alpha d}).$$

A typical result for $d = 10$, $n_0 = 0.1$ and $\alpha = 3$ is shown in Fig.2. It can be seen that for a given ringing quasiperiod d there is a set of σ which splits the edges by TV value. If we choose σ in the marked range, we can distinguish edges with ringing artifacts from edges without it.

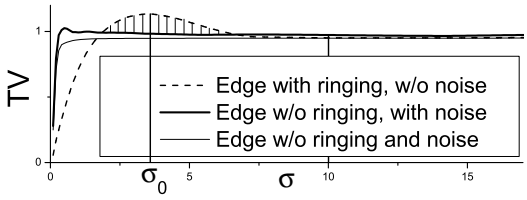

Figure 2: Scale-space TV analysis for the step edge with quasiperiod $d = 10$, maximum noise level $n_0 = 0.1$ and $\alpha = 3$ (number of oscillations ~ 3). Value $g_*(\sigma, d)$ is the maximal value of the TV of the step edge without ringing effect (thick solid line), $g^*(\sigma, d)$ is the minimal value of the TV of the step edge with ringing effect (dash line).

So we found the scale $\sigma_0(d)$ that corresponds to the maximal gap between $g^*(\sigma, d)$ and $g_*(\sigma, d)$:

$$\sigma_0(d) = \arg\max_{\sigma} (g_d^*(\sigma, d) - g_*(\sigma, d)).. \tag{2}$$

The calculated values of σ_0 for $n_0 = 0.1$ and $\alpha = 3$ for different d are shown in Fig.3. For low quasiperiods d, there is no σ such that $g^*(\sigma, d) > g_*(\sigma, d)$, another words, we cannot distinguish the edges with ringing effect from the edges without ringing effect for given n_0 and α by analyzing the TV. Ringing effect can be reasonable detected by the proposed method only for $d > d_{min}$. The value d_{min} depends on noise level n_0: for higher noise values d_{min} is greater. The analysis of d_{min} is a subject of future work.

The function $\sigma_0(d)$ is close to linear function and we use an approximation

$$\sigma_0(d) = m_{\alpha, n_0} d.$$

For $\alpha = 3$ and $n_0 = 0.1$, good approximation is $m_\alpha = 0.35$.

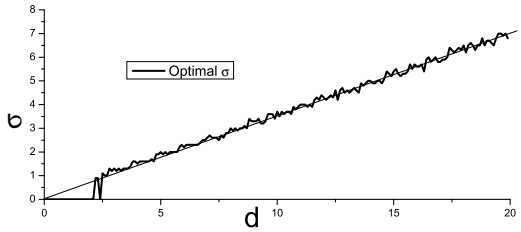

Figure 3: The results of σ_0 calculation (2) for $n_0 = 0.1$ and $\alpha = 3$ for different d. Thin line is a linear approximation of function $\sigma_0(d)$.

Experiments also show that m_α does not depend too much on α for reasonable range of α ($2 < \alpha < 5$). For the case $\alpha \leq 2$ the above algorithm does not give stable results.

2.4 Edge Ringing Level Estimation

This enables us to consider the value

$$R_E^*(f,d) = TV(f, m_\alpha d, w_{\alpha d})$$

as edge ringing level. For the case of edges with an arbitrary height, we perform a normalization. For $\sigma = d$, the values $g_*(\sigma)$ and $g_d^*(\sigma)$ are close, so it is natural to divide the value R_E^* by $TV(f, d, w_{\alpha d})$. Ringing value takes the form:

$$R_E(f,d) = \frac{TV(f, m_\alpha d, w_{\alpha d})}{TV(f, d, w_{\alpha d})}.$$

To make a decision about the presence of ringing effect, we compare the calculated ringing level R_E with threshold functions

$$G_*(d) = g_*(m_\alpha d, d),$$
$$G^*(d) = g^*(m_\alpha d, d).$$

If $R_E \geq G^*(d)$, we assume that the edge has ringing artifact. If $R_E \leq G_*(d)$, we assume that the edge does not have ringing artifact. The decision in the case $G_*(d) < R_E < G^*(d)$ needs additional analysis for each specific image class.

The calculated threshold functions $G_*(d)$ and $G^*(d)$ for $n_0 = 0.1$ and $\alpha = 3$ for different d are shown in Fig.4.

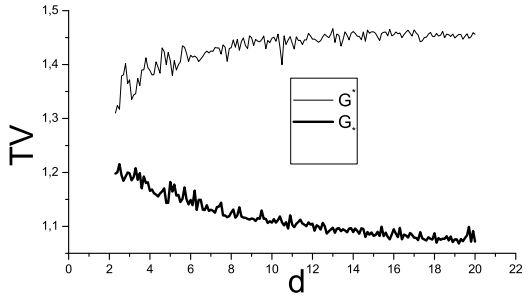

Figure 4: Threshold functions $G_*(d)$ and $G^*(d)$ for $n_0 = 0.1$ and $\alpha = 3$ for different d.

2.5 Ringing Quasiperiod Estimation and Edge Width Analysis

In real situations, we do not know the information about ringing quasiperiod d. This value has to be estimated, but we do not directly estimate d. Instead of this, we calculate edge width w and take this value as an approximation of ringing quasiperiod $d = w$. Using edge width instead of ringing quasiperiod enables to perform ringing level estimation even if ringing artifact is absent. Thus, edge width is considered as possible ringing quasiperiod.

The term 'edge width' does not have a certain definition. The simplest approach used in [1] is to find local minimum and local maximum near the edge center. This approach does not provide stable results for blurred and noisy edges. In [12], the edge is modeled by a special function, but it does not fit our needs.

For one-dimensional edge

$$\overline{f}(x) = \begin{cases} f_0, & x \leq x_0, \\ f_0 + \frac{(f_1 - f_0)(x - x_0)}{x_1 - x_0}, & x_0 < x < x_1, \\ f_1, & x \geq x_1 \end{cases} \qquad (3)$$

we define edge width as $w(\overline{f}) = x_1 - x_0$.

To define edge width for an arbitrary edge $f(x)$, we approximate it by the edge $\overline{f}(x)$ (3). We seek for minimum f_0 and maximum values f_1 of $f(x)$ in a neighborhood of the edge center, reducing for simplicity the edge to the case $f_0 = 0$, $f_1 = 1$.The size of this neighborhood is chosen a priori and represents the maximum considered edge width.

Next we seek for coordinates of intersections of $y = f(x)$ with $y_0 = 1/4$ and with $y_1 = 3/4$, draw a line through these points and find x_0 and x_1 as it is shown in Fig.5. In the case of multiple intersections we take the average of intersection points. We consider the obtained value as the edge width estimation.

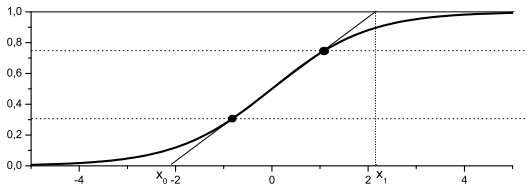

Figure 5: Edge width estimation illustration. For the shown case, the estimated edge width is 4.3 pixels.

3. 2D IMAGE RINGING LEVEL ESTIMATION

Ringing effect is located near sharp edges. It is natural to make a decision about ringing effect by analyzing the areas near sharp edges. So, we estimate image ringing level using the analysis of ringing level of 1D normal cross-sections of image edges obtained by an edge detection algorithm. General purpose edge detection algorithms do not give suitable edges for ringing level analysis. We pose the following statements for edge detection:

1. In the proposed ringing level estimation method, we consider ringing oscillations as parts of the main edge. Thus, ringing oscillations must be distinguished from the main edges.

2. If two sharp edges are positioned closely, ringing effect is interfered. We consider only distant edges to minimize the interference effect. Thus, the edges must be distant enough from each other.

3.1 Basic Edges Selection

We introduce an edge selection algorithm that follows the posed above statements. We call it basic edges selection.

To satisfy the first condition, we use the results of scale-space ringing analysis. The experiments have shown that for σ greater than edge ringing quasiperiod d, the value $TV(f_d * G_\sigma)$ becomes close to 1. It means that if we perform Gauss filtering with radius σ, ringing effect of edges with quasiperiod $d < \sigma$ will be suppressed and edge detection algorithms will not detect false edges along main edges. Thus, we perform Gauss filtering with $\sigma = d$ before edge detection. We use Canny edge detector [13] which uses Gauss filtering.

Parameter d is unknown. To estimate d, we perform Canny edge detection with predefined parameters and analyze edge widths. We consider the case of uniform high-frequency truncation for the whole image. Because d is defined by the cut-off frequency, it is constant for every edge. We approximate d using the analysis of edge widths $w_P = w(f_P(x))$, where $f_P(x)$ is edge normal cross-section function which corresponds to edge point P. For ideal edge

with ringing artifact without noise (1), $w(f_d) = d$, but real edges are not ideal. Blurred edges results in $w_P > d$, noisy edges introduce errors in w_P estimation. To estimate d with taking into account noise and blur outliers, we use the approach from our previous work [14] based on the analysis of density function of w_P distribution.

Using the estimation for ringing quasiperiod d, we take only the edges with w_P close to d: $|\frac{w_P}{d} - 1| > q$ to remove blurred edges and noisy edges with wrongly estimated edge width. Good results are achieved with $q = 0.2$.

Second condition is satisfied by calculating the distance between the edges. To make this, we construct a skeleton M_S of non-edge area and calculate the distance $\rho_P = \rho(P, M_S)$ from edge points to the skeleton. Next, we discard the edge points P with $\rho_P < \alpha d$, where α controls the number of considered ringing oscillations. The distance is calculated using Euclidean Distance Transform (EDT). The details of EDT and skeletonization are presented in following sections.

3.2 Image Ringing Level Estimation

Basic edges selection algorithm gives a set of basic edge points M_{BE} of sharp distant edges. Edge cross-sections f_P have edge width close to the estimated image ringing quasiperiod d. We define image ringing level as the average value of edge ringing values of these edge cross-sections:

$$R_E = \frac{1}{\|M_{BE}\|} \sum_{P \in M_{BE}} R_E(f_P, d),$$

where $\|M_{BE}\|$ is a number of basic edge points.

To improve the algorithm, we take only the first N edge points with maximal gradient value. Eliminating the edges with low gradient value results makes the algorithm more stable to noise and reduces the number of calculations. We use $N = 50$.

The effectiveness of the proposed algorithm of ringing level estimation for synthetic images is demonstrated in [14].

3.3 Euclidean Distance Transform

The distance transform (DT) is a general operator forming a basis of many methods in computer vision and geometry. It finds for each image pixel its smallest distance to the region of interest M:

$$D(p) = \min_{q \in M} \rho(p, q). \quad (4)$$

The simplest metrics used in DT (4) are l_1 metrics (Manhattan distance) $\rho_1(p, q) = |p_x - q_x| + |p_y - q_y|$ and l_∞ (checkerboard distance) $\rho_\infty(p, q) = \max(|p_x - q_x|, |p_y - q_y|)$. The DT for these metrics is calculated easily. These metrics do not preserve distance values during image rotation. A more natural metrics is l_2 metrics (Euclidean distance) $\rho_2(p, q) = \sqrt{(p_x - q_x)^2 + (p_y - q_y)^2}$. DT with Euclidean distance is called the Euclidean distance transform (EDT). Many fast algorithms for the EDT with linear complexity were developed in two past decades. A survey of these algorithms is given in [15]. We use Meijster's algorithm.

Numerical example of the EDT is shown in Fig.6.

3.4 Skeletonization

The idea of skeletonization is to construct a thin version of a shape that is equidistant to its boundaries.

We perform non-iterative skeletization using EDT. As the area of interest M, we take the edges, and then find all local maximum points of the EDT in horizontal, vertical and two diagonal directions. These points provide a good approximation of the skeleton. Additional skeleton post-processing like regularization or pruning does not significantly change the results of our algorithm of edges selection.

0	0	0	0	0	0	0	0	0
0	0	0	0	0	0	0	0	0
0	0	0	1	1	1	0	0	0
0	0	1	1	1	1	1	0	0
0	0	1	1	1	1	1	0	0
0	0	1	1	1	1	1	0	0
0	0	0	1	1	1	0	0	0
0	0	0	0	0	0	0	1	0
0	0	0	0	0	0	1	0	0

0	0	0	0	0	0	0	0	0
0	0	0	0	0	0	0	0	0
0	0	0	1	1	1	0	0	0
0	0	1	2	4	2	1	0	0
0	0	1	4	8	4	1	0	0
0	0	1	2	4	2	1	0	0
0	0	0	1	1	1	0	0	0
0	0	0	0	0	0	0	1	0
0	0	0	0	0	0	1	0	0

Figure 6: Numerical example of the Euclidean distance transform (EDT). Left figure: input data, black pixels (zeroes) form the region of interest. Right figure: the squares of the Euclidean distance of each pixel to the nearest black pixel.

3.5 Edge Selection Results

The processing algorithm is step-by-step illustrated for the images of Lena and Fish in Fig. 7-12. Ideal low-pass filter (high frequency data cut-off, first $1/8$ coefficients of Fourier series were retained) was used to produce ringing artifact. The calculated ringing quasiperiod d was found equal to theoretical quasiperiod value in both cases: $d = 8$.

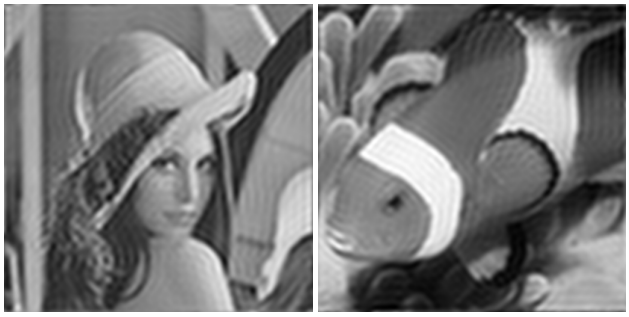

Figure 7: Input images with artificially added ringing artifact using high frequency data cut-off, first $1/8$ coefficients of Fourier series were retained.

Figure 8: Results of Canny edge detector with $\sigma = 1$ to estimate ringing quasiperiod d for the input images from Fig. 7. White edges are important edges with high gradient value. Grey edges are edges with lower gradient values. Both grey and white edges are used for skeletonization, but only white edges will be used for basic edge selection.

Figure 9: Results of Canny edge detector with Gauss radius taken in accordance with ringing quasiperiod $\sigma = d = 8$.

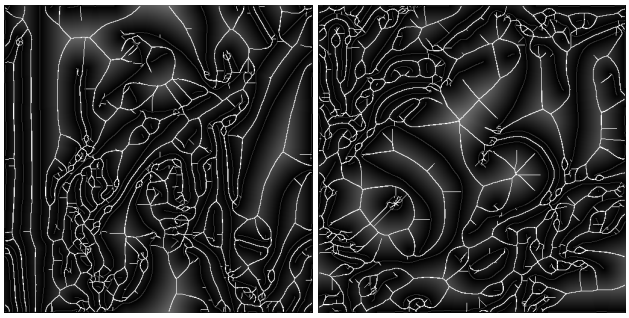

Figure 10: Skeletonization of the result of Canny edge detector from Fig.9. Background intensity level represents the distance to the edges: the higher is the intensity, the more distant to the edges is the point (EDT picture). Grey lines are the edges. White lines belong to the skeleton.

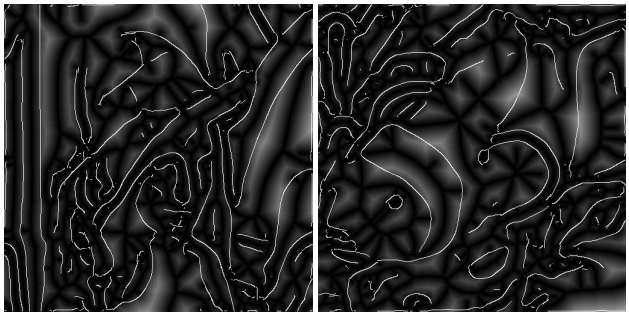

Figure 11: Calculation of the Euclidean distance from the skeleton (Fig. 10) to the edges (Fig. 9). Background intensity level represents the distance to the skeleton (EDT picture). White lines are the edges.

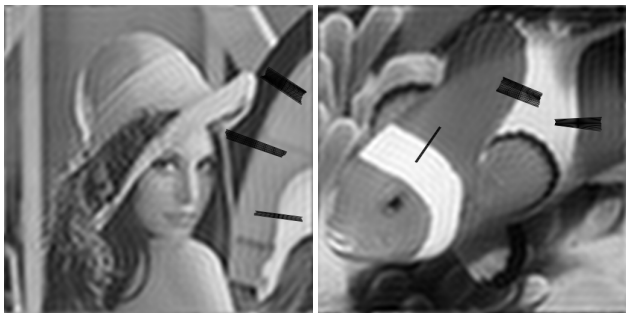

Figure 12: Results of basic edge selection for the input images. The black lines show the selected edges. The length of the line corresponding to a specific edge is equal to 6 edge widths. The number of selected edge points $N = 50$.

4. IMAGE RESTORATION QUALITY ANALYSIS METRICS

Standard metrics based on whole image square error calculation like MSE, PSNR do not correlate good enough with the perceptual image quality. As an example, ringing effect in textured areas is not noticeable while ringing effect near sharp isolated edges is annoying. We introduce an image metrics aimed at quality measurement of image restoration methods like image interpolation or image deringing in edge and edge neighborhood areas.

4.1 Basic Edges Points RMSE

To estimate the quality of edge restoration, we calculate RMSE (root of mean square error) in small neighborhood of edges points obtained by basic edges selection method:

$$BEP(u,v) = \sqrt{\frac{\sum_{M_{BEP}}(u_{i,j} - v_{i,j})^2}{\|M_{BEP}\|}},$$

where u is the reference image, v is the restored image, M_{BEP} is the edge area of the reference image u, $\|M_{BEP}\|$ is the number of points in M_{BEP}. The edge area M_{BEP} is constructed using morphological dilation of basic edges points set M_{BE} with circular structuring element with radius w:

$$M_{BEP} = \{P | \rho(M_{BE}, P) \leq w\},$$

where w is edge width. High value of BEP means that the image restoration method badly reconstructs edges, for example, introduces artifacts like blur or aliasing (jagged edges).

An example of area M_{BEP} to calculate BEP is shown in Fig.13.

4.2 Basic Edges Neighborhood RMSE

We also calculate RMSE in areas where ringing effect is the most likely to appear:

$$BEN(u,v) = \sqrt{\frac{\sum_{M_{BEN}}(u_{i,j}-v_{i,j})^2}{\|M_{BEN}\|}},$$

where M_{BEN} satisfies the condition

$$M_{BEN} = \{P | \rho(M_{BE}, P) > w, \rho(M_E, P) < \alpha w\}.$$

Here the set M_E consists of all edge points obtained by Canny edge detector in basic edges selection method. It contains all edge points from M_{BE} and edge points that do not pass the basic edges conditions and thus do not belong to basic edges.

High value of BEN means that the image restoration method works bad in edge neighborhood, for example, introduces ringing artifact.

An example of area M_{BEN} to calculate BEN is shown in Fig.13.

Figure 13: Illustration for BEN and BEP metrics. Left image is the source image. Middle image is a result of Canny edge detection. White edges are strong edges which pass the high threshold of Canny method, grey edges are weak edges which pass the low threshold. Right image shows the areas of calculation of BEP and BEN metrics. White areas are BEP areas, grey areas are BEN areas.

4.3 Image Restoration Methods Comparison

The quality of image restoration methods can be expressed in terms of the proposed basic edgse metrics. But if one method shows better BEP value, but worse BEN than another method, there is a problem to choose of the best method.

Here we introduce two methods of overall quality estimation of image restoration methods.

1. The first method constructs a relative image quality score for a set of image restoration methods. This is essential for the problem of choosing the best parameter of restoration method. Consider the values BEP_k and BEN_k as corresponding metrics values for k-th image restoration method. Next we find the maximal and minimal values of BEP_k and BEN_k:

$$BEP_* = \min_k BEP_k, \qquad BEP^* = \max_k BEP_k,$$
$$BEN_* = \min_k BEN_k, \qquad BEN^* = \max_k BEN_k.$$

We use the following rules to construct image quality score (basic edges relative quality, $BERQ$):

a. $BERQ = 0$ for $BEP = BEP_*, BEN = BEN_*$;

b. $BERQ = 1$ for $BEP = BEP^*, BEN = BEN_*$;

c. $BERQ = 1$ for $BEP = BEP_*, BEN = BEN^*$;

d. If for two methods $BEP_1 < BEP_2$ and $BEN_1 < BEN_2$, then $BERQ_1 < BERQ_2$.

We use the following definition of $BERQ$:

$$BERQ = \frac{BEP - BEP_*}{BEP^* - BEP_*} + \frac{BEN - BEN_*}{BEN^* - BEN_*}.$$

The lower is the value of $BERQ$, the better is image quality.

2. The second method is calculation of image quality value which does not depend on considered restoration methods. This problem is raised if we have to choose the best method from only two methods. The main problem is to choose the balance between BEP and BEN. We use logarithmic approach

$$BELQ = \log_2 BEP + \log_2 BEN.$$

For better presentation, we suggest BEQ metrics which is equal to $BELQ$ minus constant value $(\log_2 BEP_* - \log_2 BEN_*)$:

$$BEQ = \log_2 \frac{BEP}{BEP_*} + \log_2 \frac{BEN}{BEN_*}$$

where BEP_* and BEN_* are the normalization constants. These constants do not affect the difference between BEQ values of different images. We choose BEP_* and BEN_* as the minimal values of BEP and BEN respectively of the results of image restoration methods for the given image.

4.4 Applications to Image Interpolation

We demonstrate use of the proposed metrics by comparison of a pair of interpolation methods. We took sinc interpolation and a nonlinear combination of sinc and bicubic methods. The combination is based on weighted sum of sinc and bicubic methods, weight coefficients are functions of local TV of source and sinc interpolated images [16].

The results of image interpolation of 'house' image are shown in Fig.14, numerical results are presented in Tab.1.

Figure 14: Interpolation of 'house' image using sinc interpolation and combination of sinc and bicubic methods.

It can be seen that BEP and BEN metrics correlates with the observed quality of the considered interpolation methods: sinc interpolation shows a little bit better results in edge areas while combined method does not introduce ringing artifact in edge neighborhood. Despite MSE is better for sinc interpolation, BEQ corresponds to overall image quality.

More results and details about combined resampling method can be found in [16].

	MSE	BEP	BEN	BEQ
Sinc interpolation	109.5	14.124	4.426	0.181
Sinc + Bicubic	112.1	14.181	3.970	0.029

Table 1: The values of metrics for the images from Fig. 14.

5. IMAGE RINGING SUPPRESSION

We consider the problem of image ringing suppression in two statements: image deringing after resampling and blind image deringing.

5.1 Image Deringing after resampling

Image resampling (interpolation) is a reconstruction of a discrete image on a denser grid. In image deringing after resampling we use the fact that the TV of ideal step edge is constant for any grid. Real images have fractal nature, the TV of real images decreases after downsampling. But most of the resampling algorithms do not take this fact into consideration. So, if after upsampling the TV increases, we assume that it is caused by ringing artifact.

The main idea of the proposed method is to project the upsampled image into the convex set of images with bounded TV:

$$z_R = \arg\min_{z \in M} \|z - z_I\|^2,$$

where $M = \{z : TV(z) \leq sTV(u)\}$, z_I is the interpolated image, u is the low-resolution image, s is the scale factor. The TV is multiplied by s in 2D case, because the number of rows and columns is proportional to s.

More detailed description of this method is presented in [5].

We illustrate the proposed method of image deringing after resampling with image resampled by regularization method [17] with small regularization parameter in Fig.15.

Figure 15: Ringing estimation for image deringing after resampling. Left image: source image upsampled by pixel replication, $R_E = 1.05$. Middle image: image interpolated by regularization-based method with low regularization [17], $R_E = 1.40$. Right image: interpolated image postprocessed by deringing after resampling, $R_E = 1.06$.

5.2 Blind Image Deringing

If the low-resolution image is unknown, we use the proposed ringing metrics to a posteriori control image ringing level. Ringing reduction is performed using the regularization method based on Tikhonov regularization [18]:

$$z_R(\gamma) = \arg\min_z \left(\|z - u\|^2 + \gamma TV(z) \right),$$

where u is the given image with ringing artifact, $\gamma > 0$ is the regularization parameter. The regularization functional is consecutively minimized with increasing γ until the ringing level R_E of the result image $z_R(\gamma)$ is below the ringing threshold G^*.

The results of blind image deringing are shown in Fig.16

Figure 16: Blind image deringing. Left image: original image with ringing effect, $R_E = 1.40$. Right image: the result of automatic deringing with ringing level control, $R_E = 1.18$.

6. CONCLUSION

Adaptive image ringing detection and ringing suppression methods basing on the scale-space ringing effect analysis were developed. Method to choose strong isolated edges which are the best suitable edges for ringing analysis was proposed and used to estimate ringing level for 2D images. New image quality metrics sensible to ringing artifact were introduced. The tests showed that these metrics are promising to be widely used in image enhancement tasks.

Future work on the proposed ringing level estimation method includes additional refinement of the ringing criterion for different image classes. More effective estimation of ringing quasiperiod and edge width is under investigation.

The work was supported by federal target program "Scientific and scientific-pedagogical personnel of innovative Russia in 2009-2013" and RFBR grant 09-07-92000-HHC.

7. REFERENCES

[1] Madhuri Khambete and Madhuri Joshi, "Blur and ringing artifact measurement in image compression using wavelet transform," *Proceedings of World Academy of Science, Engineering and Technology*, vol. 20, pp. 183–186, 2007.

[2] Tao Wang and Guangtao Zhai, "Jpeg2000 image postprocessing with novel trilateral deringing filter," *Optical Engineering*, vol. 47, pp. 027005, 2008.

[3] Jinyong Fang and Jun Sun, *Advanced Intelligent Computing Theories and Applications. With Aspects of Contemporary Intelligent Computing Techniques*, chapter Ringing Artifact Reduction for JPEG2000 Images, pp. 1026–1034, Springer Berlin Heidelberg, 2007.

[4] Seungjoon Yang, Yu hen Hu, Truong Q. Nguyen, and Damon L. Tull, "Maximum-likelihood parameter estimation for image ringing-artifact removal," *IEEE Trans. Circuits Syst. Video Technol*, vol. 11, pp. 963–973, 2001.

[5] Andrey Krylov and Andrey Nasonov, "Adaptive total variation deringing method for image interpolation," *Proceedings of ICIP'08*, pp. 2608–2611, 2008.

[6] Pina Marziliano, Frederic Dufaux, Stefan Winkler, and Touradj Ebrahimi, "Perceptual blur and ringing metrics: application to jpeg2000," *Signal Processing: Image Communication*, vol. 19, pp. 163–172, 2004.

[7] T. Kartalov, Z. A. Ivanovski, L. Panovski, and L. J. Karam, "An adaptive pocs algorithm for compression artifacts removal," *9th International Symposium on Signal Processing and Its Applications*, pp. 1–4, 2007.

[8] Hantao Liu, Nick Klomp, and Ingrid Heynderickx, "Perceptually relevant ringing region detection method," *16th European Signal Processing Conference Proceedings*, 2008.

[9] Bo-Xin Zuo, "Perceptual ringing metric to evaluate the quality of images restored using blind deconvolution algorithms," *Optical Engineering*, vol. 48, no. 3, pp. 037004, 2009.

[10] L. Rudin, S. Osher, and E. Fatemi, "Nonlinear total variation based noise removal algorithms," *Physica D*, vol. 60, pp. 259–268, 1992.

[11] S. Mallat, *A Wavelet Tour of Signal Processing*, Academic Press, 1999.

[12] PeiFeng Zeng and Tomio Hirata, "Distance map based enhancement for interpolated image," *Lecture Notes in Computer Science*, vol. 2616, pp. 429–449, 2003.

[13] J. Canny, "A computational approach to edge detection," *IEEE Trans. PAMI*, vol. 8, pp. 679–714, 1986.

[14] A. V. Nasonov and A. S. Krylov, "Scale-space method of image ringing estimation," *To appear in ICIP'2009*, 2009.

[15] Ricardo Fabbri, Luciano da F. Costa, Julio C. Torelli, and Odemir M. Bruno, "2d euclidean distance transforms: a comparative survey," *ACM Computing Surveys*, vol. 40, no. 1, 2008.

[16] A. S. Krylov, A. V. Nasonov, and A. A. Chernomorets, "Combined linear resampling method with ringing control," *Proceedings of Graphicon'2009*, 2009.

[17] A. Lukin, A. Krylov, and A. Nasonov, "Image interpolation by super-resolution," *Proceedings of GraphiCon'2006*, pp. 239–242, 2006.

[18] A. N. Tikhonov and V. Y. Arsenin, *Solutions of Ill Posed Problems*, WH Winston, Washington DC, 1977.

About authors

Andrey V. Nasonov is member of scientific staff of CMC MSU.
Email: nasonov@cs.msu.ru

Andrey S. Krylov is associated professor, Head of the Laboratory of Mathematical Methods of Image Processing, CMC MSU.
Email: kryl@cs.msu.ru